

**A theoretical search on the effects of nitrogen and aluminium on  
band offset of  $\text{GaN}_x\text{As}_y\text{P}_{1-x-y}/\text{Al}_x\text{Ga}_{1-x}\text{P}$  material system.**

**M.Sc.**

**in**

**Physics Engineering**

**University of Gaziantep**

**Supervisor**

**Prof. Dr. Beşire GÖNÜL**

**by**

**Mehmet TEMİZ**

**January 2013**

©2013 [mehmet TEMİZ].

REPUBLIC OF TURKEY  
UNIVERSITY OF GAZİANTEP  
GRADUATE SCHOOL OF NATURAL & APPLIED SCIENCES  
ENGINEERING PHYSICS

Name of the thesis: A theoretical search on the effects of nitrogen and aluminium on band offset of  $\text{GaN}_x\text{As}_y\text{P}_{1-x-y}/\text{Al}_x\text{Ga}_{1-x}\text{P}$  material system

Name of the student: Mehmet TEMİZ


Exam date: 18/ 01/ 2013

Approval of the Graduate School of Natural and Applied Sciences

Assoc. Prof. Dr. Metin BEDİR

Director

I certify that this thesis satisfies all the requirements as a thesis for the degree of Master of Science.

  
Prof. Dr. A. Necmeddin YAZICI

Head of Department

This is to certify that we have read this thesis and that in our consensus/majority opinion it is fully adequate, in scope and quality, as a thesis for the degree of Master of Science.

  
Prof. Dr. Beşire GÖNÜL

Supervisor




Examining Committee Members

Signature

Prof. Dr. Beşire GÖNÜL

Assoc. Prof. Dr. Murat ODUNCUOĞLU

Assist. Prof. Dr. Hüseyin TOKTAMIŞ

**I hereby declare that all information in this document has been obtained and presented in accordance with academic rules and ethical conduct. I also declare that, as required by these rules and conduct, I have fully cited and referenced all material and results that are not original to this work.**

Mehmet TEMİZ

## ABSTRACT

A theoretical search on the effects of nitrogen and aluminium on band offset of  $\text{GaN}_x\text{As}_y\text{P}_{1-x-y}/\text{Al}_x\text{Ga}_{1-x}\text{P}$  material system.

TEMİZ, Mehmet

M.Sc. in Physics Engineering

Supervisor: Prof. Dr. Beşire GÖNÜL

January 2013, 26 pages

We present a theoretical investigation of the effect of nitrogen concentration in well and aluminum concentration in barrier on band offsets of newly proposed  $\text{GaN}_x\text{As}_y\text{P}_{1-x-y}/\text{GaP}$  and  $\text{GaN}_x\text{As}_y\text{P}_{1-x-y}/\text{Al}_z\text{Ga}_{1-z}\text{P}$  type I quantum well (QW) laser systems by means of using model Solid Theory and band anti-crossing model. We have calculated that the presence of nitrogen and aluminum improves the band alignment of the proposed novel material systems.

Key words: Band alignment and band offset, band anti-crossing model, type I quantum well.

## ÖZET

$\text{GaN}_x\text{As}_y\text{P}_{1-x-y}/\text{Al}_x\text{Ga}_{1-x}\text{P}$  materyal sisteminde Nitrojen ve Alüminyum'un band offset üzerine etkilerinin teorik araştırılması.

TEMİZ, Mehmet

Yüksek Lisans Tezi, Fizik Müh. Bölümü

Tez Yöneticisi: Prof. Dr. Beşire GÖNÜL

Ocak 2013, 26 sayfa

Yeni önerilen  $\text{GaN}_x\text{As}_y\text{P}_{1-x-y}/\text{Al}_z\text{Ga}_{1-z}\text{P}$  kuantum kuyu lazer sistemlerinde kuyu içerisindeki nitrojen ve bariyer içerisindeki alüminyumun band yönelimi üzerine olan etkilerinin Model Solid Theory ve Band anti-crossing modeli kullanarak teorik olarak araştırılıp, sunuldu. Nitrojen ve alüminyumun yeni önerilen  $\text{GaN}_x\text{As}_y\text{P}_{1-x-y}/\text{Al}_z\text{Ga}_{1-z}$  kuantum kuyu lazer sisteminin band yönelimine katkı sağladığı görüldü.

Anahtar kelimeler: Band yönelimi ve band offset, band anticrossing modeli, tip 1 kuantum kuyusu.

*I dedicate this thesis to my dear FAMILY.*

## **ACKNOWLEDGEMENTS**

It would not have been possible to write this thesis without the help and support of the kind people around me, to only some of whom it is possible to give particular mention here.

Above all, I would like to profoundly thank my supervisor, Professor Beşire GÖNÜL, for being an amazing mentor and allowing me to follow my research passions. This thesis would not have been possible without the help, support and patience of my supervisor, Prof.Dr. Beşire Gönül, not to mention her advice and unsurpassed knowledge. I also would like to thank my colleague Ömer Lütfi ÜNSAL I am particularly grateful to him, benefiting from his knowledge and our discussions about theoretical and computer subjects for all of his advice and efforts.

My special thanks to my mother and especially last father are the best parents I could ever hope for, and their prayer, love, guidance and support have been my best inspiration. My parents have given me their unequivocal support throughout, as always, for which my mere expression of thanks likewise does not suffice.



## TABLE OF CONTENTS

LIST OF TABLES.....	ii
LIST OF FIGURES.....	iii
LIST OF SYMBOLS .....	v
CHAPTER 1 .....	1
INTRODUCTION.....	1
1.1 Thesis Outline.....	3
CHAPTER 2 .....	4
THEORETICAL MODELS OF BAND STRUCTURE .....	4
2.1 Theoretical Models.....	4
2.1.1 Material parameters.....	4
2.1.2 Band Anti-crossing model .....	5
2.1.3 Model Solid Theory for unstrained semiconductors .....	8
2.1.4 Model Solid Theory for strained semiconductors .....	10
2.1.5 Interpolation method (Vegard's law) .....	12
2.1.6 Strain Effects (Zinc Blende) .....	14
MODEL CALCULATIONS AND RESULTS.....	17
3.1 Effect of Nitrogen Concentration on Band Gap of GaN <sub>x</sub> As <sub>y</sub> P <sub>1-x-y</sub> QWs on GaP substrates .....	17
3.2 Band alignment of GaN <sub>x</sub> As <sub>y</sub> P <sub>1-x-y</sub> / GaP QWs on GaP substrates.....	18
3.3 Band alignment of GaN <sub>x</sub> As <sub>y</sub> P <sub>1-x-y</sub> / Al <sub>x</sub> Ga <sub>1-x</sub> P QWs on GaP substrates.....	20
CHAPTER 4 .....	22
CONCLUDING REMARKS.....	22
LIST OF REFERENCES .....	24

## LIST OF TABLES

	<b>Page</b>
Table 2.1: Binary alloy parameters for band structure calculations.....	5

## LIST OF FIGURES

	Page
Figure 2.1: Representation in k-space of the band anticrossing effects on the nitrogen level and GaAs conduction band.....	6
Figure 2.2: Comparison between the experimentally observed and calculated band-gap reduction of GaN <sub>x</sub> As <sub>1-x</sub> as a function of N concentration.....	7
Figure 2.3: Band lineups between materials A and B in model solid theory.....	9
Figure 2.4: Band lineup of (a) compressively strained, (b) lattice matched, and (c) tensilely strained layer.....	12
Figure 2.5: Schematic diagram (a) tensile-strained and (b) compressively-strained layers grown on thick substrates.....	15
Figure 2.6: Schematic diagram showing the bulk band structure of three In <sub>1-x</sub> Ga <sub>x</sub> As ternary strained layers grown on InP substrate.....	16
Figure 2.7: Diagram of the locations of confined states in strained and unstrained Quantum Well structures. In the right and left figures, only the well material is supposed to be strained. $E_{\Gamma, hh}^w$ is the bulk band edge of the well material.....	16
Figure 3.1: The calculated variation of the strained bandgap of GaN <sub>x</sub> As <sub>y</sub> P <sub>1-x-y</sub> on GaP with increasing nitrogen concentration.....	18
Figure 3.2: The variation of the Band offset ratio of in GaN <sub>x</sub> As <sub>y</sub> P <sub>1-x-y</sub> /Al <sub>x</sub> Ga <sub>1-x</sub> P QW structure on GaP substrate with increasing nitrogen concentration.....	19
Figure 3.3: Effect of N in well and Al in barrier on band offset ratio in GaN <sub>x</sub> As <sub>y</sub> P <sub>1-x-y</sub> /Al <sub>x</sub> Ga <sub>1-x</sub> P on GaP substrates.....	19
Figure 3.4: Effect of N in well on band offset energy in GaN <sub>x</sub> As <sub>y</sub> P <sub>1-x-y</sub> /Al <sub>x</sub> Ga <sub>1-x</sub> P QW on GaP substrates.....	20

Figure 3.5: Effect of Al in barrier on band offset energy in  $\text{GaN}_{1-x}\text{As}_x\text{P}_y$  /  $\text{AlGa}_{1-x}\text{P}_y$  QW on GaP substrates.....21

## LIST OF SYMBOLS

QW	Quantum Well
BAC	Band Anticrossing Model
CB	Conduction Band
VB	Valence Band
CBM	Conduction-band Minimum
DOS	Density of State
LED	Light Emitting Diode
SC	Solar Cell
ZB	Zinc Blende
$E_g$	Band gap
$a_o$	Lattice constant
$a_e$	Lattice constant of epitaxial layer
$a_s$	Lattice constant of substrate
$T_o$	Temperature
$k_B$	Boltzmann's constant
$\Delta_o$	Spin-orbit Splitting
$a_c$	Hydrostatic deformation potential for conduction band
$a_v$	Hydrostatic deformation potential for valence band
$C_{11}$	Elastic Stiffness Constant
$C_{12}$	Elastic Stiffness Constant
$d$	Deformation Potential
$E_{v,av}$	The average valence subband energy
$\Delta E_{c,v}$	The band discontinuities for conduction and valence band
$E_c$	Conduction band energy (eV)
$E_v$	Valence band energy (eV)
$Q_{c,v}$	The band offset ratio for conduction and valence band
$\delta E_c(x,y)$	The shifted conduction band energy
$E_M$	Conduction state of the matrix semiconductor
$E_N$	Localized nitrogen state energy

$V_{MN}$	The matrix element describing the coupling effect
$C_{MN}$	Coupling constant
$E_{\pm}$	Conduction band energy state
$m_s$	Spin-split-off band
$k$	Wavevector
$E_{c-hh}$	The strained energy in the conduction band

## CHAPTER 1

### INTRODUCTION

Semiconductors are so important for device applications of electronics and optoelectronics in technology. After the possibility of alloying, different semiconductor alloys could be produced which have new fundamental and electronic properties. For example, GaAs and AlAs lattice matched binary semiconductors can be alloyed and one can produce AlGaAs which has different characteristics from GaAs and AlAs [1].

Alloying semiconductors with large size-mismatched atoms induces unusual electronic properties that can be exploited in a range of otherwise unavailable applications, such as long wavelength lasers and high performance solar cells (SC) [2]. In recent years, prominent physical and technical attention has been paid to the study of dilute nitride III-V alloys, owing to their potential optoelectronic applications devices and their unique N-induced physical properties. In III-V semiconductors, the replacement of a few percent of the group V element by small, highly electronegative and isoelectronic nitrogen atoms results in a dramatic reduction of fundamental band gap of approximately 100 meV per atomic percent of nitrogen. This enables the band gap of the resulting dilute III-V nitride alloys to be tuned to particular energies for optoelectronic applications by changing the nitrogen content. Since only small amounts of nitrogen are required to produce large changes in the band gap, the material, enabling high quality alloys to be grown epitaxially and incorporated into the existing optoelectronic infrastructure. It is known that nitrogen is an isovalent impurity which differs unmatched in size and electronegativity from other group V elements [3]. If the nitrogen impurity states lie resonantly in the conduction band a strong red shift of the fundamental band gap occurs.

The anticrossing interaction between localized nitrogen states and the extended states of the semiconductor matrix splits the conduction band into two subbands:  $E_+$  and  $E_-$  [3, 4]. The lower  $E_-$ -subband determines the fundamental band gap. The anticrossing behaviour has opened a wide possibility for the fabrication of long wavelength lasers and light emitting diodes (LED) in the 1.3–1.55  $\mu\text{m}$  range using (GaIn)(NAs) on GaAs substrate [5]. Band-gap engineering is achieved in these alloys by incorporating a small amount of nitrogen.

During the past decade, dilute nitrides, particularly the quaternary material system of III-N-V have attracted a great deal of attention, both because of unusual physical properties and potential applications in a variety of optoelectronic devices.

The dominance of silicon as a low cost material for electronic circuit applications has led to a desire to combine the advantages of optical data processing with the mature silicon microelectronics technology [6]. This merging of technologies is essential to keep up with the ever increasing need for bandwidth in optical inter- and intra-chip connections [7]. The significance of this emerging technology has made it an active area of investigation within both the industrial [8-10] and academic sectors [11-13]. However, the key challenge using silicon as a monolithic integration platform is the lack of a silicon based laser. The indirect band gap of silicon causes inefficient light emission. On the other hand, the large lattice mismatch between silicon and conventional III/V laser materials like GaAs[14-15] or InP[16] leads to difficulties in growing defect-free or threading dislocation free laser materials on silicon substrates. The quaternary dilute nitride GaNAsP material shows a direct electronic bandgap, efficient optical gain [17], and a lattice constant similar to that of silicon, [18] and is promising for the lattice-matched growth of lasers based upon this material on silicon substrate.

There are many studies on III-N-V alloys on GaAs and InP substrates, there has been no paper published yet, up to our knowledge, explaining the band alignment of III-N-V alloys on GaP and Si substrates. There is an increasing interest towards novel quaternary dilute nitride Ga(NAsP)/GaP as a promising laser material system due to their direct electronic bandgap for the As-rich regime. In this thesis study, we therefore aim to reveal the band alignment of novel direct band gap material dilute N-



containing GaAsP semiconductor alloys on GaP substrates as a function of nitrogen concentration. We also try to investigate the corresponding variations in the band alignment of novel material system of Ga(NAsP) with  $\text{Al}_z\text{Ga}_{1-z}\text{P}$  barriers as a function of Al concentration.

## 1.1 Thesis Outline

Chapter 1 provides a brief introduction to the material system under investigation. This chapter also emphasize the importance of these newly proposed material system of  $\text{GaN}_x\text{As}_y\text{P}_{1-x-y}$  well with GaP or  $\text{Al}_x\text{Ga}_{1-x}\text{P}$  barriers on GaP and hence on Si substrates.

We gave brief description of the theories used in calculations like model solid theory, band anti crossing model and interpolation method in chapter 2. The band structure and material parameters which are used throughout the thesis for III-V nitride QW laser systems are also provided.

Chapter 3 presents the calculated results of the band alignment of  $\text{GaN}_x\text{As}_y\text{P}_{1-x-y}$  well with GaP or  $\text{Al}_x\text{Ga}_{1-x}\text{P}$  barriers on GaP and hence on Si substrates. A brief discussions of the obtained results are also provided.

Finally, chapter 4 summarizes the concluding remarks and future work.

## CHAPTER 2

### THEORETICAL MODELS OF BAND STRUCTURE

The aim of this chapter is to describe and express several models, which are related to the band structure properties and material parameters of the QW laser system.

#### 2.1 Theoretical Models

A theoretical model is a theory designed to explain an entire situation or behaviour, with the idea that it would eventually be able to predict that behaviour.

##### 2.1.1 Material parameters

In theoretical model's calculations, material parameters have a significant mission. Linear interpolation is employed to calculate the lattice constant, effective masses, elastic stiffness constants and strain-related parameters of the conventional ternary and quaternary materials. [19]. The constant values of the related binary alloys are tabulated in table 2.1.

Band structure material parameters are the most important commonly measured and calculated ones and they include [19]:

- I. Direct and indirect energy gap.
- II. Crystal-field splitting for nitrides
- III. Spin-orbit splitting.
- IV. Luttinger parameters and split-off hole mass.

- V. Electron effective mass. Conduction and valence band deformation potentials that account for strain effects.
- VI. Band offsets on an absolute scale which allows the band alignments between any combinations of materials to be determined.

Table 2.1: Binary alloy parameters for band structure calculations [20 - 22].

<b>Material</b>	<b>GaAs</b>	<b>GaN</b>	<b>GaP</b>	<b>AlP</b>
Lattice Constant, $a_0(\text{\AA})$	5.6533	4.5	5.450	5.467
Energy gap, $E_g(\text{eV})$	1.424	3.299	2.76	3.63
Spin-orbit Splitting, $\Delta_o(\text{eV})$	0.34	0.017	0.08	0.07
Hydrostatic deformation potential for CB, $a_c$ (eV)	-7.17	-6.71	-8.2	-5.7
Hydrostatic deformation potential for VB, $a_v$ (eV)	-1.16	-0.69	-1.7	-3.0
Elasti Stiffness Constant, $C_{11}$ (GPa)	1221.0	293.0	1405	1330.0
Elasti Stiffness Constant, $C_{12}$ (GPa)	566.0	159.0	620.3	630.0
Deformation Potential, $b$ (eV)	-2.0	-2.0	-1.6	-1.5
$E_{v,av}$	-6.92	0.0	-7.40	-8.09

### 2.1.2 Band Anti-crossing model

Although conventional semiconductors have the tendency of increasing band gap energy with decreasing lattice constant, in the III-N-V system there is a

striking reduction in fundamental band gap energy and a huge increase in electron effective mass. Shan et al [23] have shown that these unconventional behaviours can be quite well understood within a simple Band Anti-crossing (BAC) model.

The proposed model has specific importance since, despite its plainness, it manages to explain the basic properties of the material and to provide analytical expressions, such as conduction band edge dispersion relations and electron effective mass. The BAC has been successfully used to define the dependences of the upper and lower subband energies on nitrogen concentration. The model is based upon the interaction of the lowest conduction band with the highly localized N-induced energy level  $E_N$ .

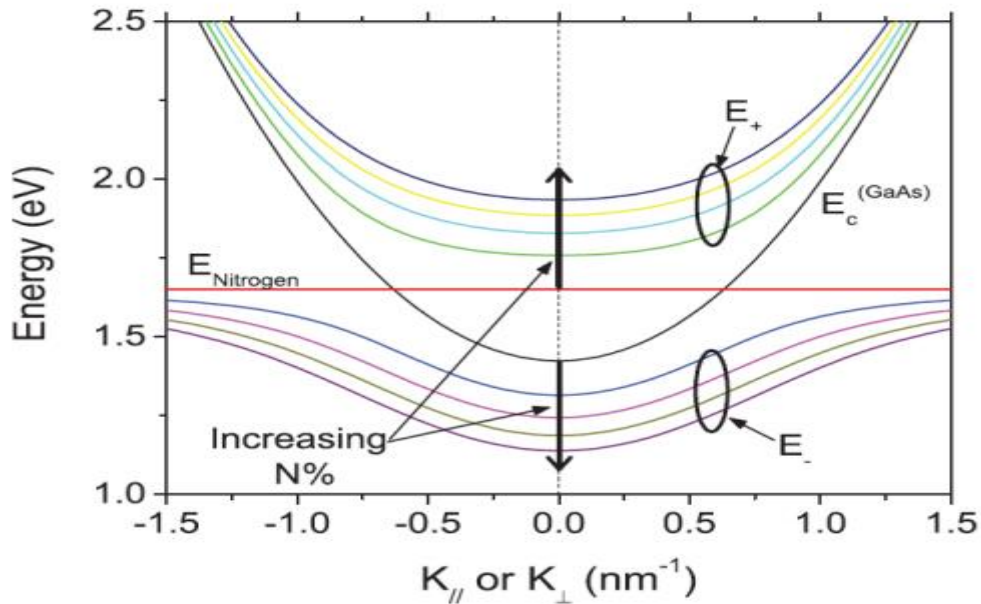


Figure 2.1: Representation in  $k$ -space of the band anti-crossing effects on the nitrogen level and GaAs conduction band [24].

It has been shown that an anti-crossing interaction of the localized N states with the extended state of GaAs, see Fig. 2.1, or GaInAs leads to a characteristic splitting of the conduction band into two non-parabolic subbands[23].

The relation between the extended conduction states of the matrix semiconductor (i.e. GaAs is matrix semiconductor for  $\text{GaN}_x\text{As}_{1-x}$  alloy) and the localized N states is treated as a perturbation which leads to the following eigenvalue problem

$$\begin{vmatrix} E - E_M & -V_{MN} \\ -V_{MN} & E - E_N \end{vmatrix} \quad (2.1)$$

where  $E_M$  is the conduction states of the matrix semiconductor,  $E_N$  is the localized nitrogen state energy (relative to the top of the valence band) and  $V_{MN}$  is the matrix element describing the interaction between these two states. Incorporation of the interaction represented by the matrix element  $V_{MN}$  leads to a mixing and anti-crossing of these states [25] equal to;

$$V_{MN} = C_{MN} \sqrt{y} \quad (2.2)$$

where  $C_{MN}$  is the coupling constant and  $y$  is the N composition. The solution to this eigenvalue problem gives us the dispersion relation

$$E_{\pm} = \frac{E_N + E_M \pm \sqrt{(E_N - E_M)^2 + 4V_{MN}^2}}{2} \quad (2.3)$$

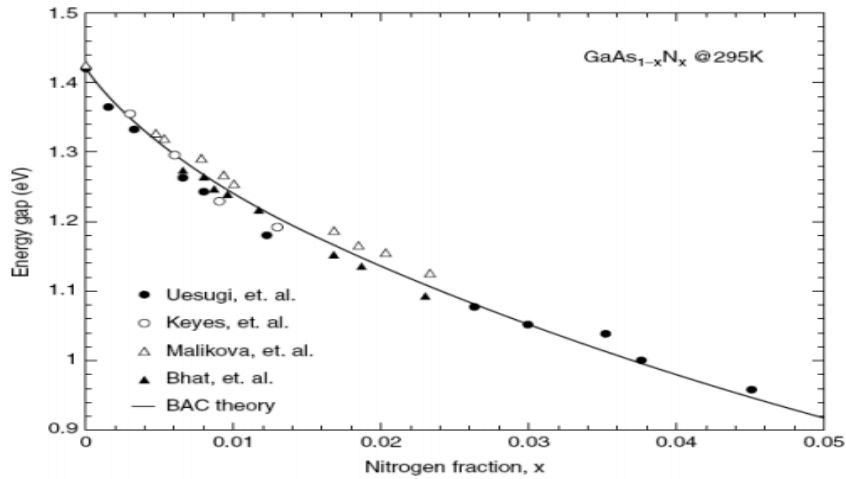


Figure 2.2: Comparison between the experimentally observed and calculated band-gap reduction of  $\text{GaN}_x\text{As}_{1-x}$  as a function of N concentration [26].

The predicted splitting of the conduction band into subbands has been confirmed experimentally as can be seen from the Fig. 2.2 [26]. The BAC model provides simple analytic expressions for the conduction band dispersion as a function of N concentration and allows to calculate, for example, the strength of the optical transitions [27] in bulk materials and the transition energies between electronic states in quantum wells or the gain in laser structures [28].

### 2.1.3 Model Solid Theory for unstrained semiconductors

The model-solid theory was first proposed by van de Walle and Martin [29-31], followed by others [32-34] to calculate strain effects on the band lineups. The relative band alignment of the band edges between quantum well and barrier is the total band discontinuity distributed over the conduction and valence bands,  $\Delta E_c$  and  $\Delta E_v$ , respectively. The band discontinuity depends on the semiconductors and the amount of mismatch strain at the interface. According to Van de Walle's model solid theory [29], the band offset ratio for conduction and valence band,  $Q_{c,v}$ , is determined by discontinuity fractions of  $\Delta E_{c,v}/\Delta E_g$ . The energy of the potential barrier,  $\Delta E_g$  is determined from the difference between the bulk bandgap energy of the barrier layers and the strained bandgap energy of the active layer.

If material A and B have the same lattice constants, we may have an ideal heterojunction and there is no strain in the semiconductors. For this case, the heavy hole and light-hole band edges ( $E_{HH}$  and  $E_{LH}$ ) are degenerate at the zone center, and their energy position is denoted as  $E_v$ :

$$E_v = E_{v,av} + \frac{\Delta}{3} \quad (2.4)$$

where  $\Delta$  is the spin-orbit splitting energy, and the spin-orbit split-off band edge energy  $E_{so}$  is

$$E_{so} = E_v - \Delta = E_{v,av} - \frac{2\Delta}{3} \quad (2.5)$$

The conduction band edge is obtained by adding the band-gap energy  $E_g$  to  $E_v$ :

$$E_c = E_v + E_g \quad (2.6)$$

Note that in the model-solid theory, the spin-orbit splitting energy  $\Delta$  and the band gap energy  $E_g$  are taken from experimental results. The band lineups between materials A and B are shown in Fig.2.3.

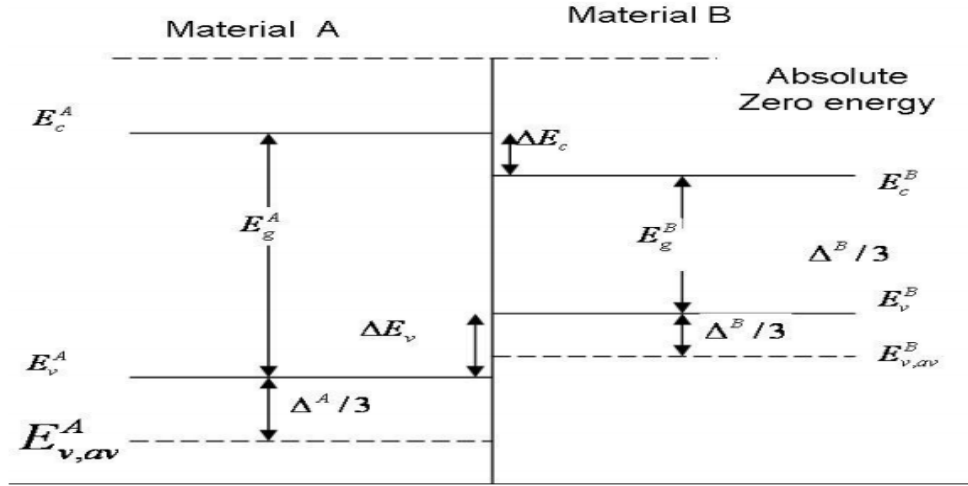


Figure 2.3: Band lineups between materials A and B in model solid theory [20].

The band gap difference is

$$\Delta E_g = E_g^A - E_g^B \quad (2.7)$$

and the band-edge discontinuities are

$$\Delta E_v = E_v^B - E_v^A \quad (2.8)$$

$$\Delta E_c = E_c^A - E_c^B \quad (2.9)$$

$$\Delta E_g = \Delta E_c + \Delta E_v \quad (2.10)$$

The band offsets ratios of the band-edge discontinuities for conduction and valance bands, respectively,

$$Q_c = \Delta E_c / \Delta E_g \quad (2.11)$$

$$Q_v = \Delta E_v / \Delta E_g \quad (2.12)$$

### 2.1.4 Model Solid Theory for strained semiconductors

The band discontinuity depends on the semiconductors and the amount of mismatch strain at the interface. According to Van de Walle's model solid theory [29] the energy of the potential barrier,  $\Delta E_g$ , is determined from the difference between the bulk band gap energy of the barrier layers and the strained band gap energy of the active layer.

The conduction band position can be calculated by simply adding the strained bandgap energy to the valence band position. The unstrained valence band-edge of the active region material is set as the reference energy of zero. The valence band position is given by

$$E_v(x, y) = \begin{cases} E_{v,av}(x, y) + \frac{\Delta_0(x, y)}{3} + \delta E_{hh}(x, y) \\ E_{v,av}(x, y) + \frac{\Delta_0(x, y)}{3} + \delta E_{lh}(x, y) \end{cases} \quad (2.13)$$

where  $E_{v,av}(x, y)$  is the average valence subband energy and  $\Delta_0$  is the spin-orbit split-off band energy.

The conduction band is shifted by the energy  $\delta E_c(x, y)$

$$\delta E_c(x, y) = 2a_c \left(1 - \frac{C_{12}}{C_{11}}\right) \varepsilon \quad (2.14)$$

where  $\varepsilon = \frac{a_s - a_e}{a_e}$  with  $a_s$  is the lattice constant of the substrate and  $a_e$  is the lattice

constant of the well material. The valence bands are shifted by energy,  $\delta E_{hh}(x, y)$  and  $\delta E_{lh}(x, y)$

$$\delta E_{hh}(x, y) = -P_\varepsilon - Q_\varepsilon \quad (2.15)$$

$$\delta E_{lh}(x, y) = -P_\varepsilon + Q_\varepsilon \quad (2.16)$$

where

$$P_\varepsilon = -2|a_v| \left(1 - \frac{C_{12}}{C_{11}}\right) \varepsilon \quad (2.17)$$



$$Q_\varepsilon = -b \left( 1 + 2 \frac{C_{12}}{C_{11}} \right) \varepsilon \quad (2.18)$$

where  $a_c$  and  $a_v$  are the conduction- and valence-band hydrostatic deformation potentials,  $b$  is the valence band shear deformation potential and  $C_{11}$  and  $C_{12}$  are elastic stiffness constants. The absolute value of hydrostatic deformation potential for valence band,  $a_v$ , is used to reconcile differing sign conventions found in literature [35, 36]. The strained band gaps can then be expressed as

$$E_{c-hh}(x, y) = E_g(x, y) + \delta E_c(x, y) - \delta E_{hh}(x, y) \quad (2.19)$$

$$E_{c-lh}(x, y) = E_g(x, y) + \delta E_c(x, y) - \delta E_{lh}(x, y) \quad (2.20)$$

The conduction band position is

$$E_c(x, y) = \begin{cases} E_v(x, y) + E_{c-hh}(x, y) & \text{for } -hh \\ E_v(x, y) + E_{c-lh}(x, y) & \text{for } -lh \end{cases} \quad (2.21)$$

The conduction band offset is given by

$$\frac{\Delta E_c}{\Delta E_g} = 1 - \frac{E_v^w - E_v^b}{E_g^b - E_g^w} \quad (2.22)$$

where  $E_v^w$  and  $E_v^b$  are the valence band positions in the well and barrier materials, respectively, and  $E_g^w$  and  $E_g^b$  are the strain adjusted bandgaps ( $E_{c-hh}$ , for compressive strain and  $E_{c-lh}$ , for tensile strain) for the well and barrier materials.

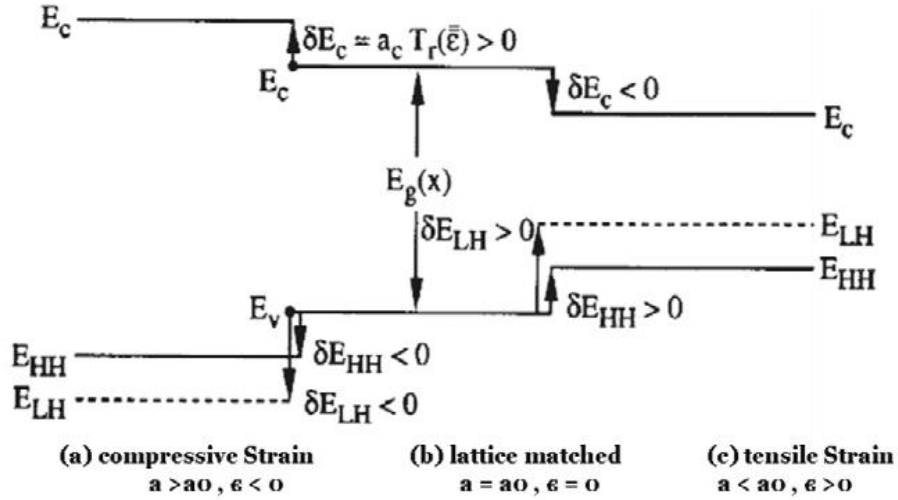


Figure 2.4: Band lineup of (a) compressively strained, (b) lattice matched, and (c) tensilely strained layer [37].

### 2.1.5 Interpolation method (Vegard's law)

Optoelectronic devices often employ alloys of binary materials. Because of the random distribution of elements from the same group within the alloy lattice, exact calculations of material parameters are hardly possible. The most important parameters of a semiconductor are the band gap and the lattice constant. To calculate the lattice constant of semiconductor alloys, Vegard's law is usually employed [24]. It states that the lattice constant of a semiconductor alloy is calculated by a linear interpolation between the lattice constant of the constituent semiconductor. If one uses linear interpolation, the ternary material parameter (T) can be derived from binary parameters (B's) by

$$T_{ABC}(x) = xB_{AC} + (1-x)B_{BC} \quad (2.23)$$

for alloy of the form given by  $A_x B_{1-x} C$ .

Some material parameters, however, deviate largely from the linear relation of Eqn.( 2.23), ternary parameter, in such case, can be very efficiently approximated by the relationship of

$$T_{ABC}(x) = xB_{AC} + (1-x)B_{BC} - Cx(x-1) \quad (2.24)$$

The parameter C is usually called a “bowing” or “non linear” parameter. For most III-V alloy bandgap is typically smaller than the linear interpolation result and so C is positive.

The quaternary material  $A_{1-x}B_xC_yD_{1-y}$  is thought to be constructed of four binaries: AC, AD, BC, and BD. If one uses a linear interpolation scheme, the quaternary parameter (Q) can be derived from the binary parameters by

$$Q(x, y) = (1-x)yB_{AC} + (1-x)(1-y)B_{AD} + xyB_{BC} + x(1-y)B_{BD} \quad (2.25)$$

If relationships for the ternary parameters (T's) are available, the quaternary parameter can be expressed either as ( $A_{1-x}B_xC_yD_{1-y}$ )

$$Q(x, y) = \frac{x(1-x)[yT_{ABC}(x) + (1-y)T_{ABD}(x)] + y(1-y)[xT_{ACD}(y) + (1-x)T_{BCD}(y)]}{x(1-x) + y(1-y)} \quad (2.26)$$

or

$$Q(x, y) = \frac{xyT_{ABD}(u) + y(1-x-y)T_{BCD}(v) + x(1-x-y)T_{ACD}(w)}{xy + y(1-x-y) + x(1-x-y)} \quad (2.27)$$

with

$$\begin{aligned} u &= \frac{(1-x-y)}{2} \\ v &= \frac{(2-x-2y)}{2} \\ w &= \frac{(2-2x-y)}{2} \end{aligned} \quad (2.28)$$

For the quinary  $A_{1-x}B_xC_yD_{1-y-z}E_z$ , the average can be expressed in terms of the nine ternary alloys (ABC, ABD, BCD, ACD, ACE, BCE, ADE, ABE and BDE):

$$P_{ABCDE} = \frac{\sum C_{ijk} P_{ijk}}{\sum C_{ijk}} \quad (2.29)$$

where  $C_{ijk}$  are the fractional composition components, e.g.  $C_{ijk} = xy(1-y-z)$  for BCD.

### 2.1.6 Strain Effects (Zinc Blende)

The lattice parameters of the semiconductor materials constituting the well and the barrier are different in the relaxed materials. If one grows a thin layer of the well semiconductor on a thick layer of the barrier semiconductor, the barrier semiconductor imposes its lattice parameter in the well plane. It is thus possible to grow elastically strained quantum wells in compression or tension. The epilayer is under a biaxial stress such that its in-plane lattice constant  $a_{||}$  equals the substrate lattice constant  $a_s$ . For the purposes of this thesis growth along the (001) direction is only considered. The net strain in the layer plane  $\epsilon_{||}$  is given by

$$\epsilon_{||} = \epsilon_{xx} = \epsilon_{yy} = \frac{a_s - a_e}{a_e} \quad (2.30)$$

In response to the biaxial stress, the layer relaxes along the growth direction, the strain  $\epsilon_{\perp}$  ( $= \epsilon_{zz}$ ) being of opposite sign to  $\epsilon_{||}$  and given by

$$\epsilon_{\perp} = -2 \frac{\sigma}{1 - \sigma} = -2 \frac{2C_{12}}{C_{11}} \epsilon_{||} \quad (2.31)$$

where  $\sigma$  is the Poisson's ratio and  $C_{11}$  and  $C_{12}$  are elastic stiffness constants. For compressive strain,  $a_e < a_s$ ,  $\epsilon_{xx} = \epsilon_{yy} < 0$ , and  $\epsilon_{zz} > 0$ . The total strain can be resolved into a purely axial component,  $\epsilon_{ax}$ , given by:

$$\epsilon_{ax} = \epsilon_{\perp} - \epsilon_{||} \approx -2\epsilon_{||} \quad (2.32)$$

and a hydrostatic component  $\epsilon_{vol}$  ( $= \Delta V/V$ ), given by:

$$\epsilon_{vol} = \epsilon_{xx} + \epsilon_{yy} + \epsilon_{zz} \approx \epsilon_{||} \quad (2.33)$$

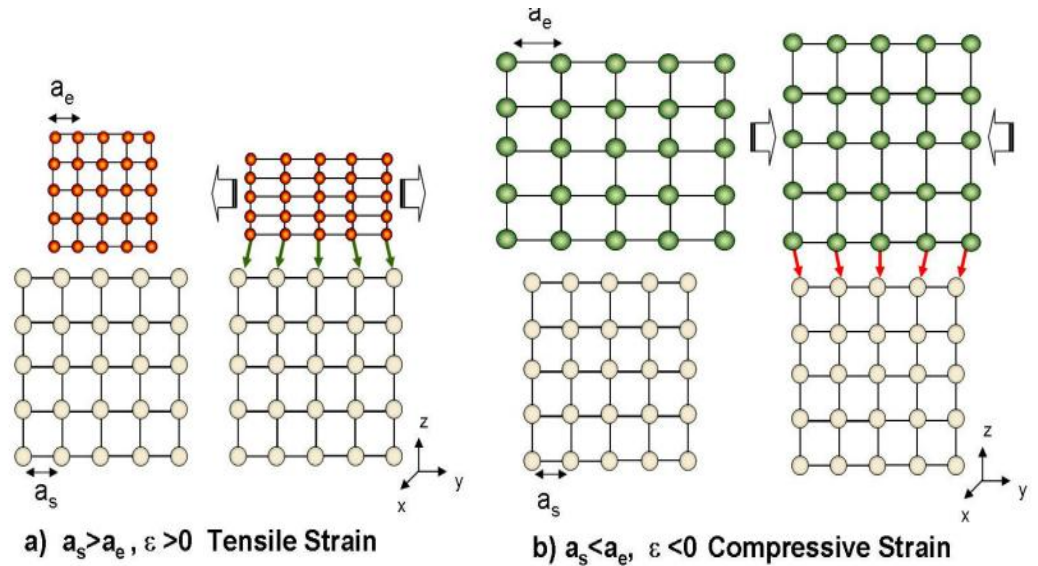


Figure 2.5: Schematic diagram (a) tensile-strained and (b) compressively-strained layers grown on thick substrates.

The resolution of the strain into components is important when modelling the effects of strain on the band structure of semiconductors. The strain is then a new degree of freedom available to optimize the semiconductor laser, characteristics: the structural modifications with respect to a bulk, relaxed semiconductor, added to the size quantization effects, lead to drastic changes of the electronic properties.

Fig. 2.6 shows that in a compressively strained structure, the heavy hole, light-hole splitting at  $k=0$  increases and the heavy-hole effective mass decreases. This leads to the reduction of the hole density of states, DOS, and thus to a reduction of the threshold current density. Moreover, the light-hole states, which do not participate in the lasing transition, are further in energy from the heavy-hole states compressively strained structures compared to the unstrained one. These states are thus less populated, which leads to an increase of the semiconductor laser efficiency. One can also demonstrate that the differential gain is higher in a strained structure than in a lattice matched one.

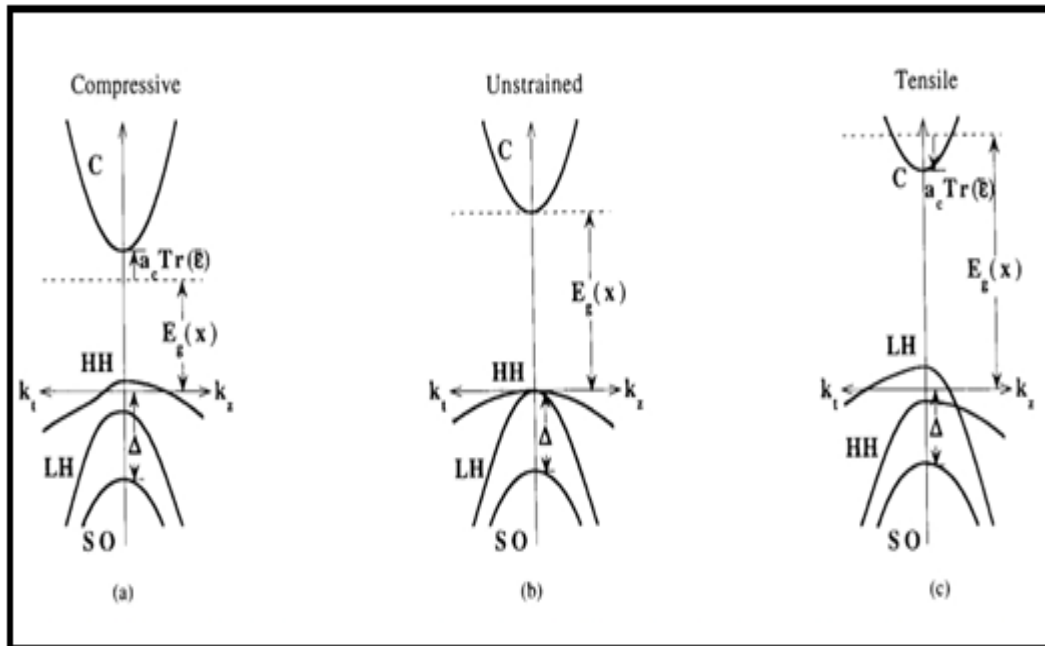


Figure 2.6: Schematic diagram showing the bulk band structure of three  $\text{In}_{1-x}\text{Ga}_x\text{As}$  ternary strained layers grown on InP substrate [38].

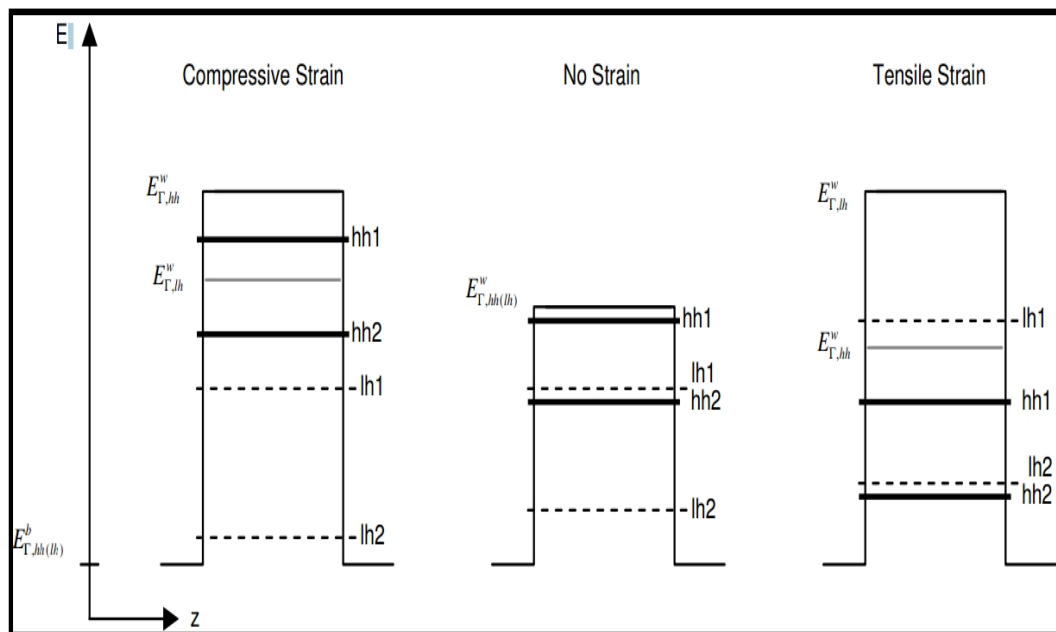


Figure 2.7: Diagram of the locations of confined states in strained and unstrained Quantum Well structures. In the right and left figures, only the well material is supposed to be strained.  $E_{\Gamma, hh}^w$  is the bulk band edge of the well material [39].

## CHAPTER 3

### MODEL CALCULATIONS AND RESULTS

Based on the theories mentioned chapter 2, we present here a theoretical comparison of band alignment of  $\text{GaN}_x\text{As}_y\text{P}_{1-x-y}/\text{GaP}$  and  $\text{GaN}_x\text{As}_y\text{P}_{1-x-y}/\text{Al}_z\text{Ga}_{1-z}\text{P}$  QWs on GaP substrates. The novel quaternary well material of GaNAsP exhibits a direct band gap only for the As-rich regime [18]. The lattice constant of the quaternary GaNAsP can be adjusted to fit the GaP or Si by means of varying N- and P-concentration [18]. It has been shown experimentally that the lasing operation has been observed in these novel GaNAsP material system based on GaP[40]. We investigate the effect of nitrogen in well and Al in barrier on band alignment (band offset energy and ratio) in  $\text{GaN}_x\text{As}_y\text{P}_{1-x-y}/\text{Al}_x\text{Ga}_{1-x}\text{P}$  QW structure on GaP substrate.  $\text{GaN}_x\text{As}_y\text{P}_{1-x-y}$  forms well and  $\text{Al}_x\text{Ga}_{1-x}\text{P}$  forms barrier of our quantum well (QW). In well N, As, and P all belong to group V of the periodic table.

#### 3.1 Effect of Nitrogen Concentration on Band Gap of $\text{GaN}_x\text{As}_y\text{P}_{1-x-y}$ QWs on GaP substrates

The growth of GaNAsP on GaP substrates results in compressive strain. The magnitude of the compressive strain increases with increasing (decreasing) arsenide (phosphide) concentration. We have calculated the strained band gap of  $\text{GaN}_x\text{As}_y\text{P}_{1-x-y}/\text{GaP}$  by means of using band anti-crossing model which allows us to calculate the fundamental band gap,  $E_g$ . Strain effects has also been taken into account. Fig. 3.1 shows the calculated results. It has been seen from these calculations that when nitrogen concentration increases there will be a stronger repulsion between the extended state  $E_M$  and the localized N level  $E_N$  leading to a red shift in the strained band gap as shown in Fig.3.1. Band gap decreases within 100 meV for a 1% nitrogen concentration. The band anti-crossing parameter of  $C_{MN}$  which is the coupling

parameter determined by the strength of coupling between localized and extended states is taken as 1.9 [41].  $E_N$  was determined by interpolation of isolated N level in ternary composition end points of GaAs:N and GaP:N [42]. The nitrogen dependence of the conduction band energy  $E_M$  of the matrix semiconductor is taken as  $E_M = E_0 - 3.5x$  [42] and  $E_0$  is the bulk band gap energy in the absence of nitrogen.

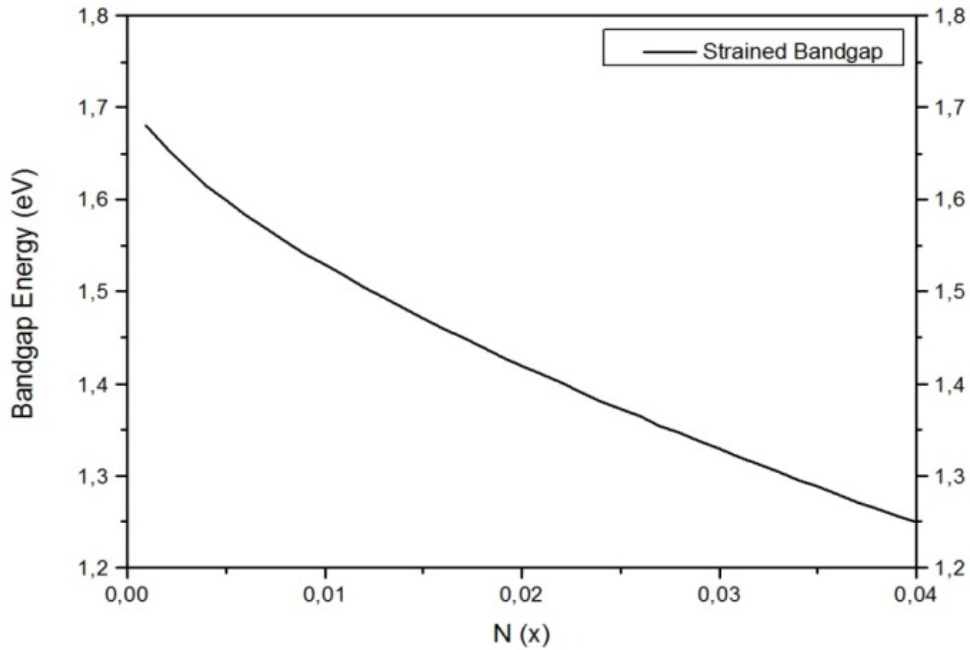


Figure 3.1: The calculated variation of the strained bandgap of  $\text{GaN}_x\text{As}_y\text{P}_{1-x-y}$  on GaP with increasing nitrogen concentration.

### 3.2 Band alignment of $\text{GaN}_x\text{As}_y\text{P}_{1-x-y}$ / GaP QWs on GaP substrates

We investigate the band alignment, i.e. band offset ratios and energies, by means of using Model Solid Theory. Fig. 3.2 presents the calculated band offset ratios ( $Q_c$  and  $Q_v$ ) for compressively strained As-rich  $\text{GaN}_x\text{As}_{0.8}\text{P}_{0.2-x}$  quantum well with GaP barriers on GaP substrates. Upper curve represents the variation of the conduction band offset ratio  $Q_c$  and lower curve represents the valence band offset ratio  $Q_v$  with increasing nitrogen concentration in well. An arsenide concentration of 80% has been chosen to keep the well material in direct band gap region. These calculations show that the introduction of N into GaAsP increases the conduction band offset ratio  $Q_c$  and decreases the valence band offset ratio  $Q_v$  gradually. Fig. 3.3 illustrates the corresponding band offset energies for compressively strained As-rich



$\text{GaN}_x\text{As}_{0.8}\text{P}_{0.2-x}$  quantum well with GaP barriers on GaP substrates. It has been seen from Fig. 3.3 that N incorporation increases both conduction- and valence-band offset energies leading better carrier confinement.

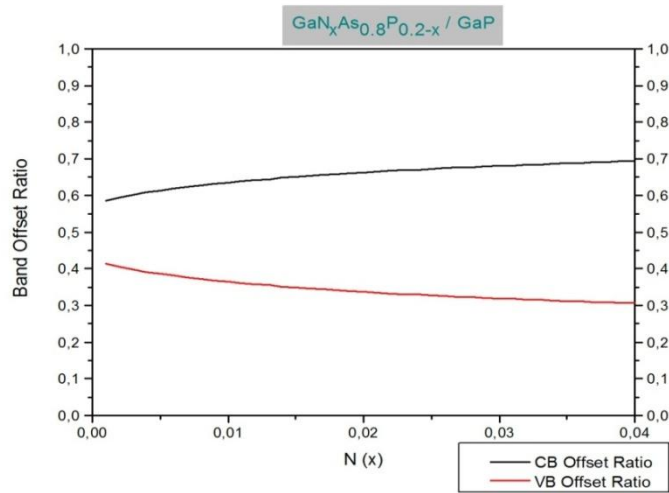


Figure 3.2: The variation of the band offset ratios of in  $\text{GaN}_x\text{As}_y\text{P}_{1-x-y}/\text{GaP}$  QW structure on GaP substrate with increasing nitrogen concentration.

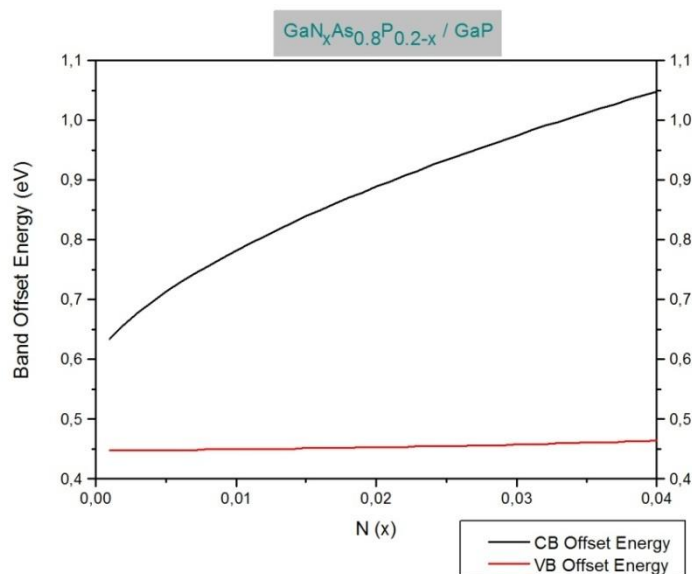


Figure 3.3: Effect of N in well on band offset energy in  $\text{GaN}_x\text{As}_y\text{P}_{1-x-y}/\text{GaP}$  QW on GaP substrates.

### 3.3 Band alignment of GaN<sub>x</sub>As<sub>y</sub>P<sub>1-x-y</sub> / Al<sub>x</sub>Ga<sub>1-x</sub>P QWs on GaP substrates

This section provides an optimization of the quaternary GaN<sub>x</sub>As<sub>y</sub>P<sub>1-x-y</sub> well material on GaP substrates by means of using Al<sub>x</sub>Ga<sub>1-x</sub>P barriers instead of GaP barriers. We therefore now investigate the effect of nitrogen in well and aluminium in barrier on the band alignment of GaN<sub>x</sub>As<sub>y</sub>P<sub>1-x-y</sub>/Al<sub>x</sub>Ga<sub>1-x</sub>P QW structure on GaP substrate. GaN<sub>x</sub>As<sub>0.8</sub>P<sub>0.2-x</sub> forms well and Al<sub>x</sub>Ga<sub>1-x</sub>P forms barrier of our quantum well (QW) structure. Fig. 3.4 presents the corresponding variation of the band offset ratio of GaN<sub>x</sub>As<sub>0.8</sub>P<sub>0.2-x</sub>/Al<sub>x</sub>Ga<sub>1-x</sub>P QW. As can be seen from Fig. 3.4, there is a significant increase in conduction band offset ratio and decrease in valence band offset ratio with increasing Al concentration in barrier.

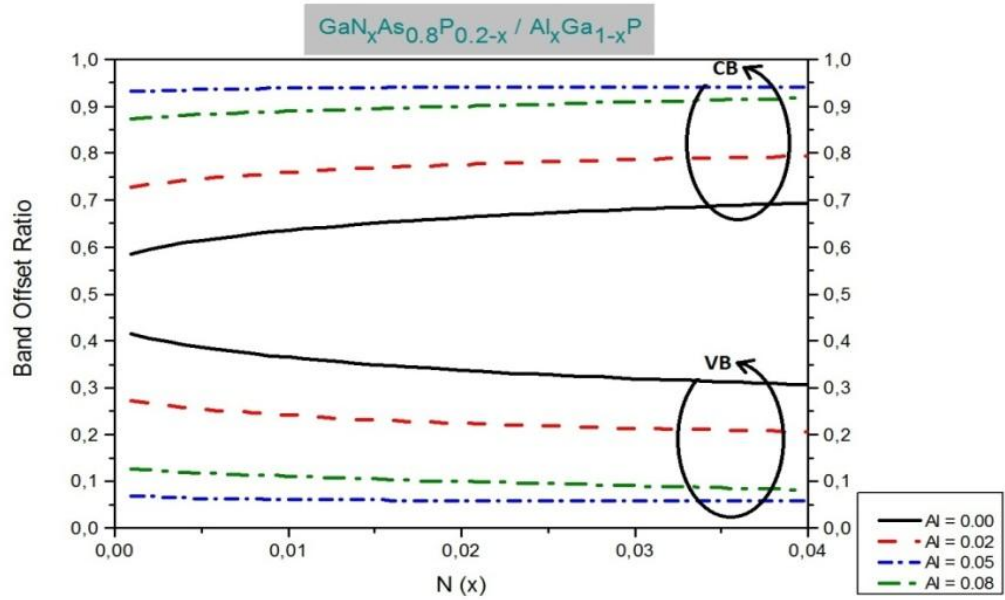


Figure 3.4: Effect of N in well and Al in barrier on band offset ratio in GaN<sub>x</sub>As<sub>y</sub>P<sub>1-x-y</sub>/Al<sub>x</sub>Ga<sub>1-x</sub>P on GaP substrates.

It should be noticed from the variations of Fig.3.4 that although the increase in conduction band offset ratio  $Q_c$  and the decrease in valence band offset ratio  $Q_v$  is slow with increasing N concentration in well, the rate of change of  $Q_c$  and  $Q_v$  are very rapid with increasing aluminum concentration in barrier. Fig.3.5 shows the corresponding the band-offset energies in the case of Al<sub>x</sub>Ga<sub>1-x</sub>P barriers. As can be seen from Fig. 3.5, it is possible to get deeper conduction and valence wells leading to

much better confinement both in conduction and valence bands. So, the use of  $\text{Al}_x\text{Ga}_{1-x}\text{P}$  barriers instead of GaP barriers improves the band alignment since band offset energies further increases with an increase of Al concentration in barrier.

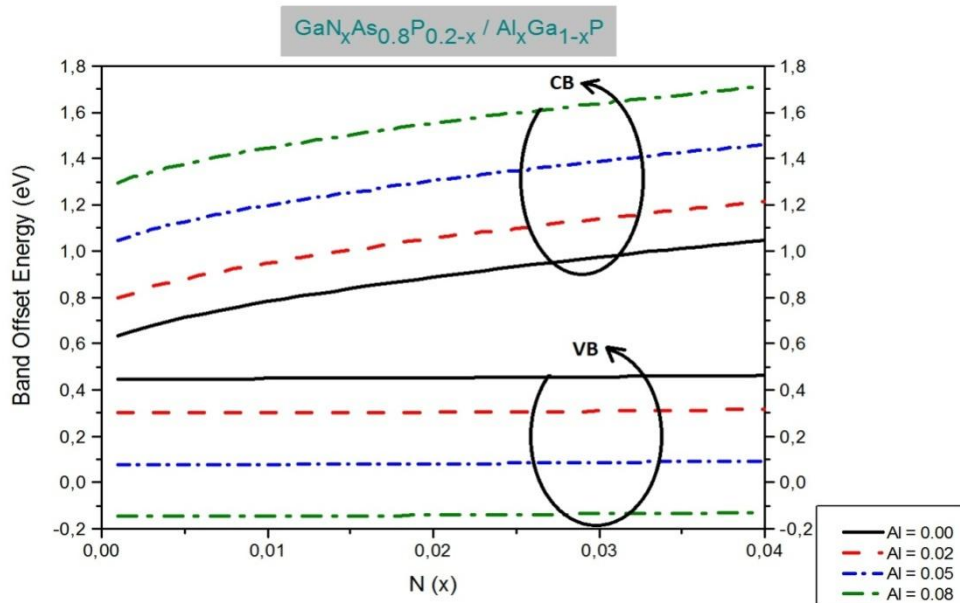


Figure 3.5: Effect of Al in barrier on band offset energy in  $\text{GaN}_x\text{As}_y\text{P}_{1-x-y} / \text{Al}_x\text{Ga}_{1-x}\text{P}$  QW on GaP substrates.

It should also be noticed from Fig. 3.5 that band offset energy becomes negative for 8% Al concentration. This means that  $\text{GaN}_x\text{As}_y\text{P}_{1-x-y} / \text{Al}_x\text{Ga}_{1-x}\text{P}$  QWs on GaP substrates turns from being type I to type II for stated Al concentration.

## CHAPTER 4

### CONCLUDING REMARKS

The III-N-V alloys has been considered as new material systems because of their unusual behaviour. These alloys grown on GaAs and InP substrate conventionally. Nevertheless these growths result strained materials and great interest must be paid while growing them. In recent years, people have considered GaP as a barrier material. The utilization of GaP brings benefits since GaP is almost lattice-matched to silicon. Hence, one can use the most available material, Si, as a substrate material in  $\text{GaN}_x\text{As}_{0.8}\text{P}_{0.2-x}$  / GaP QW laser systems.

This thesis provides a study on the band alignment of the quaternary direct band gap novel well material system of  $\text{GaN}_x\text{As}_{0.8}\text{P}_{0.2-x}$  with GaP or  $\text{Al}_z\text{Ga}_{1-z}\text{P}$  barriers on GaP substrates. We investigate the effect of N in well and Al in barrier on band offset energies and band offset ratios in  $\text{GaN}_x\text{As}_y\text{P}_{1-x-y}$ /GaP and  $\text{GaN}_x\text{As}_y\text{P}_{1-x-y}$ / $\text{Al}_x\text{Ga}_{1-x}\text{P}$  QW systems. We have calculated that the band offset energies and ratios increases with an increase of N in well of  $\text{GaN}_x\text{As}_y\text{P}_{1-x-y}$ /GaP material system. We have also calculated that the band offset energies and ratios increases with an increase of Al in barrier of  $\text{GaN}_x\text{As}_y\text{P}_{1-x-y}$ / $\text{Al}_x\text{Ga}_{1-x}\text{P}$  QW systems. Our calculations show that the rate of increase of band offset ratio and energy for conduction band is rapid than that of those in valence band. This is a desirable situation since electrons must confine better than holes in order to reduce the carrier leakage to the barrier. Electrons have a higher probability to leak to the barrier since the effective mass of the electron is smaller than that of the hole. Therefore, lighter electrons are more mobile than that of heavier holes. Hence electrons have a high probability to leak into the barrier. This carrier leakage can be reduced with better band alignment, i.e with deeper conduction wells. Our calculations show that the newly proposed novel  $\text{GaN}_x\text{As}_y\text{P}_{1-x-y}$  wells with  $\text{Al}_x\text{Ga}_{1-x}\text{P}$  barriers on GaP and hence on Si substrates

provides the requirement of carrier confinement with optimized band alignment. Therefore, the proposed novel  $\text{GaN}_x\text{As}_y\text{P}_{1-x-y}$  well with  $\text{Al}_x\text{Ga}_{1-x}\text{P}$  barrier on GaP and hence on Si substrates is a promising material system for lasers.

As a future work, it would be remarkable to investigate the effect of the incorporation of the indium into the quaternary  $\text{GaN}_x\text{As}_y\text{P}_{1-x-y}$  well with GaP or  $\text{Al}_x\text{Ga}_{1-x}\text{P}$  barriers on GaP substrates from the band alignment point of view.

## LIST OF REFERENCES

- [1] Köksal, K. (2009). Ph.D. thesis, Theoretical investigation of the effect of nitrogen on optical and electronic properties of GaInAsN semiconductors University of Gaziantep.
- [2] Veal, T. D., Mahboob, I. and McConville, C. F. (2004). Negative Band Gaps in Dilute  $\text{InN}_x\text{Sb}_{1-x}$  Alloys. *Physical Review Letters*, **92**, 136801.
- [3] Thomas, D. G., Hopfield J. J., and Frosch C. J. (1965). Isoelectronic Traps Due to Nitrogen in Gallium Phosphide. *Phys. Rev. Lett.* **15**, 857.
- [4] Shan, W., Walukiewicz, W., Ager, J. W III., Haller, E. E., Geisz, J. F., Friedman, D. J., Olson, J. M. and Kurtz, S. R. (1999). Band Anticrossing in GaInNAs Alloys. *Phys. Rev Lett.* **82**, 1221.
- [5] Perkins, J. D., Mascarenhas, A., Zhang, Y., Geisz, J. F., Friedman, D. J., Olson, J. M. and Kurtz, S. R. (1999). Nitrogen-Activated Transitions, Level Repulsion, and Band Gap Reduction in  $\text{GaAs}_{1-x}\text{N}_x$  with  $x < 0.03$ . *Phys. Rev. Lett.* **82**, 3312.
- [6] Wu, J., Walukiewicz, W., Yu, K.M., Shan, W., Ager III, J.W., Haller, E.E., Hai, L.U., Schaff, W.W., Metzger, W.K., Kurtz, S.R., (2003). Superior radiation resistance of  $\text{In}_{1-x}\text{Ga}_x\text{N}$  alloys: a full-solar-spectrum photovoltaic material system. *Appl. Phys. Lett.* **94**, 6477.
- [7] Hilleringmann, U. and Goser, K. (1995). Optoelectronic system integration on silicon: waveguides, photodetectors, and VLSI CMOS circuits on one chip. *IEEE Trans. Electron Devices* **42**, 841.
- [8] Goodman, J. W., Leonberger, F. J. L., Kung, S.-Y. and Athale, R. A., (1984). Optical interconnections for VLSI systems, *Proc. IEEE* **72**, 850.
- [9] Paniccia, M. (2010). Integrating silicon photonics. *Nat. Photonics* **4**, 498.
- [10] Rong, H. S., Liu, A. S., Jones, R., Cohen, O., Hak, D., Nicolaescu, R., Fang, A., and Paniccia, M. (2005). An all-silicon Raman laser. *Nature (London)* **433**. 292.

- [11] Liu, H., Wang, T., Jiang, Q., Hogg, R., Tutu, F., Pozzi, F. And Seeds, A. (2011). Long-wavelength InAs/GaAs quantum-dot laser diode monolithically grown on Ge substrate. *Nat. Photonics*. **5**, 416.
- [12] Liang, D. And Bowers, J. E. (2010). Recent progress in lasers on silicon. *Nat. Photonics*. **4**, 511.
- [13] Pavesi, L., Negro, L. D., Mazzoleni, C., Franzo, G., and Priolo, F. (2000). Optical gain in silicon nanocrystals. *Nature (London)* **408**, 440.
- [14] Fang, S. F., Adomi, K., Iyer, S., Morkoc, H., Zabel, H., Choi, C. and Otsuka, N. (1990). Gallium arsenide and other compound semiconductors on silicon. *J. Appl. Phys.* **68**, R31.
- [15] Kromer, H., Liu, T. Y. and Petroff, P. M. (1989). GaAs on Si and related systems: Problems and prospects. *J. Cryst. Growth*. **95**, 96.
- [16] Saint-Girons, G., Regreny, P., Largeau, L., Patriarche, G. and Hollinger, G. (2007). Monolithic integration of InP based heterostructures on silicon using crystalline Gd<sub>2</sub>O<sub>3</sub> buffers. *Appl. Phys. Lett.* **91**, 241912.
- [17] Borck, S., Chatterjee, S., Kunert, B., Volz, K., Stolz, W., Heber, J., Rühle, W. W., Gerhardt, N. C. and Hofmann, M. R. (2006). Lasing in optically pumped Ga(NAsP)/GaP heterostructures. *Appl. Phys. Lett.* **89**, 201105.
- [18] Kunert, B., Volz, K., Koch, J. and Stolz, W. (2006). Direct-band-gap Ga(NAsP)-material system pseudomorphically grown on GaP substrate. *Appl. Phys. Lett.* **88**, 182108.
- [19] Ellmers, C., Hofmann, M., W. Rühle, W., Girndt, A., Jahnke, F., Chow, W. W. Knorr, A., Koch, S.W., Hanke, C., Korte, L., and Hoyler, C. (1999), Gain Spectra of an (InGa)As Single Quantum Well Laser Diode. *Physica Status Solidi*. **206**, 407.
- [20] Bakır, E. (2007). M.sc.thesis, Investigation of the Band Alignment of long-Wavelength InGa(N)As(Sb) Quantum wells on GaAs and InP Substrates. University of Gaziantep.
- [21] Vurgaftman, I., Meyer, J.R. and Ram, M.L.R, (2001), Band parameters for III–V compound semiconductors and their alloys. *Journal of Applied Physics*, **89**.
- [22] Vurgaftman, I. and Meyer, J.R. (2003), Band parameters for nitrogen-containing semiconductors. *Japanese Journal of Applied Physics*. **94**.

- [23] Shan, W., Walukiewicz, W., Ager III, J. W., Haller, E. E., Geisz, J. F., Friedman, D. J., Olson, J. M. and Kurtz, S. R. (1999). Band Anticrossing in GaInNAs Alloys. *Phys. Rev. Lett.* **82** 1221.
- [24] Yuen, H. B. (2006). Ph.D. thesis, Stanford Univ.
- [25] Suemune, I., Uesugi, K. and Walukiewicz, W. (2000). Role of nitrogen in the reduced temperature dependence of band-gap energy in GaNAs. *Appl. Phys. Lett.* **77** 3021.
- [26] van de Walle, C. G. and Martin, R. M. (1986). Theoretical calculations of heterojunction discontinuities in the Si/Ge system. *Phys. Rev. B.* **34**, 5621.
- [27] van de Walle, C. G. and Martin, R. M. (1987). Theoretical study of band offsets at semiconductor interfaces. *Phys. Rev. B.* **35**, 8154.
- [28] Wang, T. Y. and Stringfellow, G. B. (1990). Strain effects on Ga<sub>x</sub>In<sub>1-x</sub>As/InP single quantum wells grown by organometallic vapor-phase epitaxy with  $0 \leq x \leq 1$ . *J. Appl. Phys.* **67**, 344.
- [29] Krijn, M. P. C. M. (1991). Heterojunction band offsets and effective masses in III-V quaternary alloys. *Semicond. Sci. Technol.* **6**, 27.
- [30] Satpathy, S., Martin, R. M. and van de Walle, C. G. (1988). Electronic properties of the (100) Si/Ge strained-layer superlattices. *Phys. Rev. B* **38**, 13237.
- [31] Chuang, S. L. (1995). *Physics of Optoelectronic devices*, Godman J W New York Wiley Series in Pure and Applied Optics. 661.
- [32] Chuang, S. (1991). Efficient band-structure calculations of strained quantum wells using a two-by-two Hamiltonian. *Phys. Rev. B.* **43**, 9649.
- [33] Keith Barnham, Dimitri D Vvedensky. (2001). *Low-Dimensional Semiconductor Structures: Fundamentals and Device Applications*.
- [34] Chih-Sheng Chang and Shun Lien Chuang. (1995). *Senior Member Ieee, Ieee Journal Of Selected Topics In Quantum Electronics*, Vol. I. No. 2.
- [35] Keith, B., Dimitri, D. V. (2001). *Low-Dimensional Semiconductor Structures: Fundamentals and Device Applications*.
- [36] B. Kunert, S. Reinhard, J. Koch, M. Lampalzer, K. Volz, and W. Stolz, (2006). First demonstration of electrical injection lasing in the novel dilute nitride Ga(NAsP)/GaP-material system. *Phys. stat. sol. (c)*. **3**, 614.



- [37] Chamings, J., Adams, A. R., Sweeney, S. J., Kunert, B., Volz, K. and Stolz, W. (2008). Temperature dependence and physical properties of Ga(NAsP)/GaP semiconductor lasers. *Appl. Phys. Lett.* **93**, 101108.
- [38] Kunert, B., Volz, K. and Stolz, W. (2007). Determination and improvement of spontaneous emission quantum efficiency in GaAs/AlGaAs heterostructures grown by molecular beam epitaxy. *Phys. Stat. Sol. (B)* **244**, 2730.
- [39] Walukiewicz, W., Shan W., Wu, J., and Yu, K.M. *Band Anticrossing in III-N-V Alloys: Theory and Experiments Materials Sciences Division, Lawrence Berkeley National Laboratory, Berkeley, California.*
- [40] Perlin, P., Wisniewski, P., Skierbiszewski C., Suski, T., Kaminska, E., Subramanya, S. G., Weber, E. R., Mars, D. E. and Walukiewicz, W. (2000). *Appl. Phys. Lett.* **76**, 1279 46.
- [41] Hader, J., Koch, S. W., Moloney, J. V., and Oreilly, E. P. (2000). Influence of the valence-band offset on gain and absorption in GaNAs/GaAs quantum well lasers. *Appl. Phys. Lett.* **76**, 3685.
- [42] van de Walle, C. G. (1989). Band lineups and deformation potentials in the model-solid theory. *Phys. Rev. B.* **39**, 1871.